Neurotoxicology 75 (2019) 78–88

Contents lists available at ScienceDirect

Neurotoxicology

journal homepage: www.elsevier.com/locate/neuro

Full Length Article

Proteomic profiling of primary astrocytes and co-cultured astrocytes/microglia exposed to acrylamide

Mengyao Zhao[a,b,c], Li Dong[a], Chunfeng Zhu[c], Xiaosong Hu[a], Liming Zhao[c], Fang Chen[a,*], Hing Man Chan[b,*]

[a] College of Food Science and Nutritional Engineering, National Engineering Research Center for Fruits and Vegetables Processing, Key Laboratory of Fruits and Vegetables Processing, Ministry of Agriculture, Engineering Research Centre for Fruits and Vegetables Processing, Ministry of Education, China Agricultural University, Beijing 100083, China

[b] Department of Biology, University of Ottawa, Ottawa, Ontario K1N 6N5, Canada

[c] State Key Laboratory of Bioreactor Engineering, R&D Center of Separation and Extraction Technology in Fermentation Industry, School of Biotechnology, East China University of Science and Technology, Shanghai 200237, China

ARTICLE INFO

Keywords:
Acrylamide
Co-cultured cells
Neurotoxicity
Oxidative stress
Primary astrocytes
Proteomics

ABSTRACT

- Acrylamide (AA) is a common food contaminant known to detrimentally affect the nervous system. Homeostasis of the nervous system is dependent on glial cells, namely astrocytes and microglia, which actively participate in neuronal survival signaling pathways. Although the differential responses of monocultured astrocytes compared to co-cultured astrocytes and microglia to AA exposure have been investigated, the global effects and potential molecular mechanism involved in AA-induced neurotoxicity remain unknown. In this study, the impacts of AA on primary monocultured astrocytes and co-cultured astrocytes with microglia were determined using Orbitrap-based proteomic analysis. The results showed that AA exposure mainly caused disruption of cellular and metabolic processes, biological regulation, and cell development. Furthermore, oxidative stress-related pathways and immune responses were the main regulatory functions influenced by AA-induced neurotoxicity. Additionally, Nrf2 and other downstream proteins in the oxidative stress-related pathway were up-regulated. There were significant differences between the protein changes in the monocultured astrocytes and co-cultured astrocytes with microglia, indicating that AA affected cell-cell communication between astrocytes and microglia. Overall, these findings illustrate the global effects of AA-induced functionality and pathway alteration and their involvement in the development of neurological deficits in primary glial cell cultures. These findings may provide new insights for the development of a pathway approach suitable for the risk assessment of AA.

1. Introduction

Acrylamide (AA) is a common food contaminant that forms during the food heating process (Mottram et al., 2002; Stadler et al., 2002; Tareke et al., 2002). Since 1994, the International Agency for Research on Cancer has classified AA as probably carcinogenic to humans (Group 2A) (International Agency for Research on Cancer (IARC, 1994). Given its potential health hazard, increasing efforts by both the academic community and food industry have been devoted to risk mitigation and toxicity control of AA (Zhang et al., 2009). Classical studies indicated that high exposure to AA could cause neurotoxicity in both humans and experimental animals (Fullerton, 1969; Ralevic et al., 1991). However, the mechanisms of AA-induced neurotoxicity require clarification. In the mid-1990s, several studies examined whether AA interacted with cellular proteins to produce neurotoxicity, and showed that inactivation of these proteins suppressed nerve terminal processes and impaired neurotransmission (Abelli et al., 1991; Edwards et al., 1991). More recent *in vivo* and *in vitro* studies have demonstrated that AA attacks the active sites of presynaptic proteins, forming covalent adducts with highly nucleophilic cysteine thiolate groups (LoPachin and Barber, 2006). Additional research has indicated that AA causes neurotoxicity by inducing oxidative stress and activating cytochrome P450 2E1 (Ghanayem et al., 2005; Huang et al., 2012; Lakshmi et al., 2012); the subsequent mitochondrial dysfunction triggered by these processes

* Corresponding authors.
E-mail addresses: chenfangch@sina.com (F. Chen), laurie.chan@uottawa.ca (H.M. Chan).

https://doi.org/10.1016/j.neuro.2019.09.005
Received 11 February 2019; Received in revised form 30 August 2019; Accepted 5 September 2019
Available online 08 September 2019
0161-813X/

contributes to the neurotoxicity (Prasad and Muralidhara, 2013, 2014).

Most neurotoxicological studies of the effects of AA have focused on a specific pathway or formation of particular DNA and protein adducts. By contrast, the global neurotoxic effects of AA are not well established and warrant further research. Proteomics represents a powerful tool for toxicological assessments, as it provides comprehensive information that can be used to monitor the cellular response to environmental stimuli (Rabilloud and Lescuyer, 2015). In a previous proteomic study of AA neurotoxicity, treatment with both high and low doses of AA resulted in the formation of adducts on presynaptic cysteine-directed proteins and a dopamine transporter (Barber and LoPachin, 2004). In rats subjected to AA treatment, the results of the subsequent proteomic analysis of the striatal synaptosomes confirmed the effects on the nerve terminal proteome (Barber et al., 2007). Basile et al. (2008) developed a technique for rapid AA-hemoglobin adduct detection using a proteomic approach as a highly sensitive biological method to monitor AA toxicity. In a recent proteomic study, Martyniuk et al. (2013) reported that ˜0.7% of the N27 cell proteome involved in processes associated with atherosclerosis, inflammation, neurotoxicity, nerve degeneration, and diabetes was adducted. Based on the generic electrophilic reactivity of AA, previous studies employing a proteomic approach have focused on the chemical sites of AA-protein adduct formation. By contrast, there have been no proteomic studies of AA-induced pathway alteration.

Homeostasis of the nervous system is maintained by the main functional glial cells, namely astrocytes and microglia, which are actively involved in neuronal survival signaling (Anderson and Swanson, 2000; Streit et al., 1998). Both oxidative stress and immune response reportedly result from exposure to various environmental contaminants, such as titanium dioxide, trimethyltin, methylmercury, and acrylonitrile. Furthermore, these pollutants alter the related signaling pathways in astrocytes and microglial cells, eliciting dose- and time-dependent responses (Caito et al., 2014; Kuhlmann and Guilarte, 2000; Long et al., 2007; Ni et al., 2011). Previous research has suggested the presence of cell-specific responses to AA exposure, with astrocytes and microglia showing distinct sensitivity (Zhao et al., 2017a, 2017b). Considering these findings and the different functions of astrocytes and microglia in the central nervous system, we employed proteomic analysis for the continued investigation of the global neurotoxic effects of AA in both isolated astrocytes and astrocytes co-cultured with microglia.

The goal of this study was to use a label-free proteomic approach to investigate AA-induced differential protein expression and subsequent modifications to biological functions and pathways in primary mono-cultured astrocytes and co-cultured astrocytes and microglia. Moreover, the differences in the responses and functional changes between the two cell culture systems were investigated.

2. Methods

2.1. Materials

BALB/c mice were obtained from Charles River (Montreal, QC, Canada). AA was purchased from Sigma-Aldrich (Oakville, ON, Canada). Minimum Essential Medium with Earle's balanced salt solution (MEM/EBSS with 2 mM L-glutamine), Hank's Balanced Salt Solution (HBSS), phosphate-buffered saline, 0.25% trypsin-EDTA, and penicillin/streptomycin (10,000 U/mL) were acquired from GE Life Sciences (Logan, UT, USA). Heat-inactivated fetal bovine serum (FBS) was obtained from Thermo Fisher Scientific (Gibco, Australia origin, Catalog #10100147; endotoxin level ≤ 10 EU/mL; hemoglobin level ≤ 30 mg/dL). CD11b microbeads and magnetic columns were obtained from Miltenyi Biotec (Auburn, CA, USA). The Pierce Mass Spec Sample Prep Kit was purchased from Thermo Fisher Scientific (San Jose, CA, USA). All solvents used were of at least high-performance liquid chromatography (HPLC) grade.

2.2. Cell culture and AA exposure

Research ethics approval for animal use was obtained from the Animal Care and Use Committee of the University of Ottawa according to the guidelines of the Canadian Council on Animal Care (approval code: BL-270). The primary cell cultures were prepared as described previously (Marek et al., 2008; Zhao et al., 2017a). Briefly, neonatal BALB/c mice were sacrificed via cervical dislocation within postnatal day 1–2, and the whole brains were harvested. The meninges were removed, and the remaining tissue was placed in 10 mL of HBSS containing 300 μg/mL DNase I and 0.25% trypsin. The solution was gently triturated several times using a pipet, followed by incubation in a tissue rotator at 37 °C for 40 min. The tissue was passed through a 70-mm nylon mesh strainer and centrifuged (300 × *g*, 10 min). The collected cells were re-suspended in culture medium (MEM/EBSS with 10% FBS and 1% penicillin/streptomycin) and plated at a density of two mouse brains per 75 cm^2 culturing flask. After incubation for 24 h, non-adherent cells were removed, after which the adhered cells were incubated in culture medium for 10 days, with a medium change every 3–4 days. After 10 days, oligodendrocytes were removed using complement-mediated cytolysis, and the remaining cells were incubated in culture medium for 10 days without medium change. Magnetic cell sorting was employed to separate dislodged cells using CD11b microbeads (Miltenyi Biotec, Auburn, CA, USA) according to the manufacturer's directions. The positive fraction contained purified microglial cells, whereas the negative fraction was enriched for astrocytes. Purified cells were re-suspended in culture medium for subsequent experimentation. The purity of the separated astrocytes and microglia was evaluated via immunostaining (Marek et al., 2008), as viewed under a fluorescence microscope (Olympus, Sacramento, CA, USA) (Supporting Information Fig. S1).

Primary astrocytes or a combination of microglia and astrocytes (at a 1:1 ratio) were plated onto 10-cm flat-bottomed culture plates containing culture medium (MEM/EBSS with 10% FBS and 1% penicillin/streptomycin) and cultured overnight in a humidified incubator containing 5% CO_2 and 95% air at 37 °C. The use of 1:1 ratio is to keep consistency with the study design of our previous study (Zhao et al., 2017). The following day, a complete media change was performed with AA-spiked medium. For the AA dose selection (concentration range with 1, 10, 50, 100, 500, 1000 μM), preliminary cell viability assays were performed using the MTT (3-(4,5-dimethylthiazol-2-yl)-2,5-diphenyltetrazolium bromide) assay.

2.3. Sample preparation and in-solution digestion

The protein samples were prepared according to the manufacturer's instructions using a Pierce Mass Spec Sample Prep Kit (Thermo Fisher Scientific). Briefly, an aliquot of cultured cells (≥ 1×10^6 cells) was mixed with cell Lysis Buffer (Thermo Fisher Scientific) to a final volume of 100 μL, followed by incubation at 95 °C for 5 min. The lysate was sonicated on ice to reduce the viscosity of the sample and centrifuged at 16,000 × *g* for 10 min at 4 °C. Equal amounts of lysate protein (100 μg) were added to adjust the final concentration to 1 mg/mL. Dithiothreitol was mixed into a 100-μg sample to a final concentration of 10 mM and incubated at 50 °C for 45 min. Subsequently, 11.5 μL of 500-mM iodoacetamide solution was added, followed by incubation for 20 min in the dark at room temperature. After alkylation, the sample was mixed with a 4× volume of pre-chilled (−20 °C) acetone, and incubated overnight at −20 °C to precipitate proteins. Then, the samples were centrifuged at 16,000 × *g* for 10 min at 4 °C, and the protein pellets were collected. The acetone-precipitated protein pellets were re-suspended in Digestion Buffer (Thermo Fisher Scientific) to a final volume of 100 μL. Protease trypsin was added to the sample at an enzyme: protein ratio of 1:50, and incubated overnight at 37 °C. Digestion was stopped by acidification with 5 μL of 10% trifluoroacetic acid, and the samples were cleaned with C_{18} tips (Thermo Fisher Scientific). Finally,

the specimens were re-suspended in 0.1% trifluoroacetic acid and subjected to HPLC-mass spectrometry (MS) analysis.

2.4. Label-free proteomic analysis using HPLC-MS (Orbitrap Fusion)

A Dionex UltiMate 3000 RSLCnano HPLC system coupled with an Orbitrap Fusion mass spectrometer (Thermo Fisher Scientific) coupled with an Acclaim PepMap RSLC column (75 μm ID ×150 mm; Thermo Fisher Scientific) was used for the HPLC-MS analysis of peptides. A 2-μL sample (containing 1 μg of peptides) was injected and separated with the following gradient of solvents A (0.1% formic acid in H_2O) and B (80% acetonitrile, 0.1% formic acid in H_2O) at a flow rate of 200 nL/min: 0.0–80.0 min 0–40% B, 80.0–80.1 min 40–80% B, 80.1–90.0 min 80% B, 90.0–90.1 min 80–2% B, and 90.1–115.0 min 2% B. The nano-electrospray ionization conditions were as follows: spray voltage in positive mode, 2000 V; ion transfer tube temperature, 275 °C; S-lens RF level, 60. Survey scans of peptide precursors from 300 *m/z* to 1500 *m/z* were performed at 60 K resolution (at 200 *m/z*) with a 2×10^5 ion count target and maximum injection time of 50 ms. Tandem MS was performed by isolation at 0.7 Th with the quadrupole, collision-induced dissociation fragmentation with a collision energy of 35% and a 5% step, as well as normal scan mode in the ion trap. The MS^2 ion count target was set to 10^4, and the maximum injection time was 35 ms. Precursors with a charge state of 2–6 were sampled for MS2. The dynamic exclusion duration was set to 60 s with a 10-ppm tolerance around the selected precursor and its isotopes. The instrument was operated at top speed in 4-s cycles.

2.5. Database searching

Tandem mass spectra were processed using PEAKS Studio ver. 8.0 (Bioinformatics Solutions Inc., CA, USA). A PEAKS DB was established to search the UniProt/SwissProt database (mouse version 201701) with trypsin as the digestion enzyme. The PEAKS DB was searched with a fragment ion mass tolerance of 0.05 Da and a parent ion tolerance of 7.0 ppm. Carbamidomethylation was specified as a fixed modification. Furthermore, oxidation, deamidation, and acetylation were specified as variable modifications. The relative abundance of peptide features (precursor peak area) was detected in multiple samples. Feature detection is performed separately on each sample, and then the features of the same peptide from different samples are reliably aligned together using a high-performance retention time alignment algorithm. Results were filtered with a 1% FDR searched against the database and proteins with at least one unique peptide were identified in each of the treatment groups. Normalization was performed on total ion current (TIC) of the samples, and normalized abundance is calculated from the raw abundance divided by the normalization factor. Differentially expressed proteins were identified if their fold change were over 1.5 and differed significantly according to the Mann–Whitney U test ($p < 0.05$). Group variance was tested using R software, and the results were illustrated as a heat map.

2.6. Hierarchical cluster analysis

Hierarchical cluster analysis (HCA) is an algorithmic approach used to uncover discrete groups with varying degrees of (dis)similarity in a dataset represented by a (dis)similarity matrix. This analysis was conducted using the pheatmap package (https://CRAN.R-project.org/package = pheatmap).

2.7. Ingenuity pathway analysis

Ingenuity Pathway Analysis (IPA; ver. 9; Ingenuity Systems Inc., Redwood City, CA, USA; www.ingenuity.com) was performed according to the manufacturer's instructions for further functional and pathway analysis.

2.8. Western blot analysis

Four proteins in the Nrf2 pathway, namely nuclear factor (erythroid-derived 2)-like 2 (Nrf2), catalase (Cat), glutamate-cysteine ligase regulatory subunit (Gclm), and sequestosome-1 (Sqstm1), were verified using the Western blot method to compare the quantitative changes in the proteomic data. Typical proteins were also assessed, including a copper transport protein (Atox1), heme oxygenase 1 (Hmox1), and cytochrome C (Cyto C).

Briefly, cell lysate was prepared in ice-cold RIPA buffer with a protein inhibitor cocktail tablet (Sigma, Shanghai, China). Protein samples (15–55 μg) were loaded and separated in 10 and 15% Mini-PROTEAN TGX Precast Gels (Bio-Rad, Shanghai, China). Membranes were blocked for 1 h with 5% skim milk in tris-buffered saline-Tween-20 (TBST), and incubated overnight with the following primary antibodies at 4°C (Abcam, Shanghai, China): Nrf2 (1:3000), Cat (1:2000), Gclm (1:5000), Sqstm1 (1:1000), Hmox1 (1:2000), Atox1(1:800), Cyto C (1:1000), and Gapdh (1:2000). The membranes were washed with TBST and incubated with goat anti-rabbit IgG-horseradish peroxidase secondary antibodies (1:3000) (Santa Cruz Biotechnology Inc., Dallas, TX, USA) for 1 h at room temperature. The blots were stained with Clarity Western ECL Substrate (Bio-Rad, Shanghai, China), and target bands were visualized by using a Tanon Imaging System (Model 3500, Tanon Science & Imaging Co., Shanghai, China). Moreover, the target bands were quantified using the ImageJ software (NIH Image, Bethesda, MD, USA), and the density of each band was normalized against Gapdh.

2.9. Statistical analysis

Bar graphs were created using Origin 8.0 (OriginLab, Northampton, MA, USA) and Prism 7.0 (GraphPad Software, La Jolla, CA, USA). Data from the western blots are presented as the means ± standard error. Statistical analysis was performed using the SPSS 17.0 statistical package (SPSS Inc., Chicago, IL, USA), and results with $p < 0.05$ were considered to be significantly different.

3. Results

3.1. Cytotoxicity of AA in astrocytes and co-cultured astrocyte/microglia

No significant cell death was evident in either monocultured astrocytes or co-cultured astrocytes/microglia at the investigated concentrations (1–1000 μM; $p > 0.05$; Fig. 1).

Previous studies (Doerge et al., 2005; Tareke et al., 2006) showed that daily administration of AA (approximately 1 mg/kg bw/day) to mice through drinking water (Doerge et al., 2005) resulted in around 1 μM of AA in the serum (Tareke et al., 2006). Therefore, we used 1 μM as the dosing concentration in the cell culture to represent the average food intake exposure. There is no data on human serum AA concentration as a result of among occupational exposure. However, Calleman et al. (1994) measured acrylamide hemoglobin adduct levels in 41 occupational workers employed at a acrylamide production plant and found levels as high as 13,400 pmol/g. In comparison, Kütting et al. (2009) measured hemoglobin acrylamide adduct among 749 adult nonsmokers and reported a mean concentration of 27.1 pmol/g after daily exposure. These results suggest that occupational exposure in extreme case can be about 500 times higher than that in daily exposure. Therefore, we chose 500 μM as the dose representing occupational exposure. A The results of this study shown in Fig. 1 were similar to several other studies that found no significant cell death following exposure to similar concentrations (Liu et al., 2015; Pan et al., 2017).

3.2. Protein identification

Proteomic analysis was performed in the control group, as well as

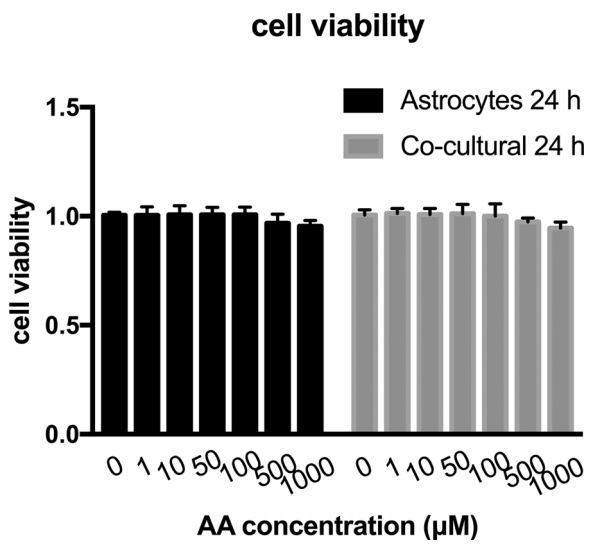

Fig. 1. Effects of 24 h acrylamide (AA) exposure on astrocyte and co-cultured astrocyte/microglial cell viability. Cell viability was measured using the MTT assay. Values are expressed as the means ± standard deviation of five independent biological replicates.

the treatment groups exposed to 1 μM (low-dose) and 500 μM (high-dose) AA using an HPLC-Orbitrap MS system. Three independent astrocytes cultures and three independent co-cultures (i.e. biological replicates) were included. Also, each biological sample included three extractions (i.e. technical replicates). Therefore, proteomic analysis was performed on a total of 18 groups of cultured cells. In order to avoid the bias of false positive identification, if a protein is below the threshold value in any of the replicates, it will be filtered out and not included in the analysis.

The list of all the identified proteins is presented in Supplement S1. A total of 3973 and 3985 proteins were identified in the astrocytes in the low and high dose groups respectively. In comparison, a total of 3974, and 3793 proteins were identified in the co-cultured cells. Only the common proteins identified in each control and AA treatment groups were included in the analysis. At the low dose treatment group, the astrocytes and co-cultured cells had 3193 proteins in common, 780 unique proteins were found in astrocytes, and 781 unique proteins were found in the co-cultured cells. At the high dose treatment group, the astrocytes and co-cultured cells had 3088 proteins in common, 897 unique proteins were found in astrocytes, and 705 unique proteins were found in the co-cultured cells.

The list of all the differentiated proteins after treatments are presented in Supplement S2. Following AA treatment in monocultured astrocytes, 7 and 22 proteins were down-regulated and up-regulated in the high-dose group; however, no significant changes were evident in the low-dose group. Therefore, only the high-dose astrocyte group was considered in the subsequent analyses. Following AA treatment in co-cultured cells, 36 and 56 proteins displayed significant changes in the low-dose and high-dose groups, respectively, compared to the control. Among these proteins, 27 were up-regulated, and 9 were down-regulated in the low-dose group, while 34 were up-regulated and 22 were down-regulated in the high-dose group ($p < 0.05$). These results indicated distinctly dissimilar responses of cells to varying concentrations of AA (Fig. 2A).

In the high-dose groups, AA exposure induced differential expression of more proteins in the co-cultured cells than monocultured astrocytes. There were only five common differentially expressed proteins found between the astrocytes and co-cultured cells. These results suggested that the biological response of astrocytes may be different when exposed to AA in the presence of microglial cells. The HCA results revealed the changes in abundance of differentially expressed proteins between the untreated control and AA-treated cells (Fig. 2B–D). The reproducibility expressed as variability between the 3 biological replicates were 78%, 79%, 80% and 83% for 1 μM Astrocytes, 500 μM Astrocytes, 1 μM co-cultured cells, and 500 μM co-cultured cells groups (after normalized to control), respectively. Nevertheless, the samples from the control and AA-treated cells displayed significant uniformity (Fig. 2B–D).

3.3. Cellular component distribution of differentially expressed proteins

The results of the cellular component distribution, according to the UniProt database are shown in Table 1. All identified proteins could be classified into eight cellular functional categories. In both monocultured astrocytes and co-cultured cells, the relative abundances of total proteins and differentially expressed proteins in the main cellular components followed the order membrane > cytoplasm > nucleus > endoplasmic reticulum > mitochondrion > Golgi apparatus > microtubule.

3.4. GO analysis of differentially expressed proteins

According to the biological processes in the UniProt database, differentially expressed proteins were classified into related functional categories (Fig. 3). From their distribution in biological processes (Fig. 3A–C), altered proteins mainly participated in three essential biological functions: (1) Cellular and metabolic process; (2) biological regulation and response to stimuli; and (3) cell development, as well as cellular component organization or biogenesis. Changes to proteins involved in cell-cell signaling accounting for 12% of the proteins (RIN1, ZNF622, APPL1, PABPN1, Cdc42ep1, Itpr2, Igfbp2) were only found in the high-dose co-cultured group (Fig. 3C). According to the molecular functions in the UniProt database, the differentially expressed proteins were classified into related functional categories (Fig. 3D–F). The molecular function terms were categorized into six main biological activities: (1) binding activity; (2) catalytic activity; (3) transporter activity; (4) signal transducer activity; (5) receptor activity; and (6) enzyme regulator activity.

3.5. IPA function and pathway analysis

For a better understanding of the functions and pathways influenced by AA, IPA was performed. The differentially expressed proteins in each AA treatment group were annotated to dozens of functional alterations. Notably, the generation of ROS and the immune response of cells were the top two ranked significant child terms for both astrocytes and co-cultured cells (Fig. 4A, B). Moreover, the analysis predicted that the formation of cellular protrusions and microtubule dynamics was activated in co-cultured cells following exposure to a high concentration of AA (Fig. 4C).

IPA enrichment analysis of differentially expressed proteins demonstrated 14, 16, and 15 pathways were changed in the high-dose astrocyte and low- and high-dose co-cultured treatments, respectively (Fig. 5). In line with the function alterations, oxidative stress-related pathways and immune response signaling were significantly enriched in both cell cultures following high-dose treatment. Moreover, the Nrf2-mediated oxidative stress response was presumed to be activated in co-cultured cells exposed to the high concentration of AA (marked as red in Fig. 5C). Finally, the downstream proteins Cat, Gclm, Txnrd1, and Sqstm1 were predicted to be up-regulated after AA exposure, contributing to Nrf2 activation (Fig. 5D).

3.6. Verification of protein expression using Western blot analysis

The Western blot results are shown in Fig. 6. According to the pathway prediction and key roles of differentially expressed proteins in co-cultured cells, proteins related to the Nrf2 pathway, including Nrf2,

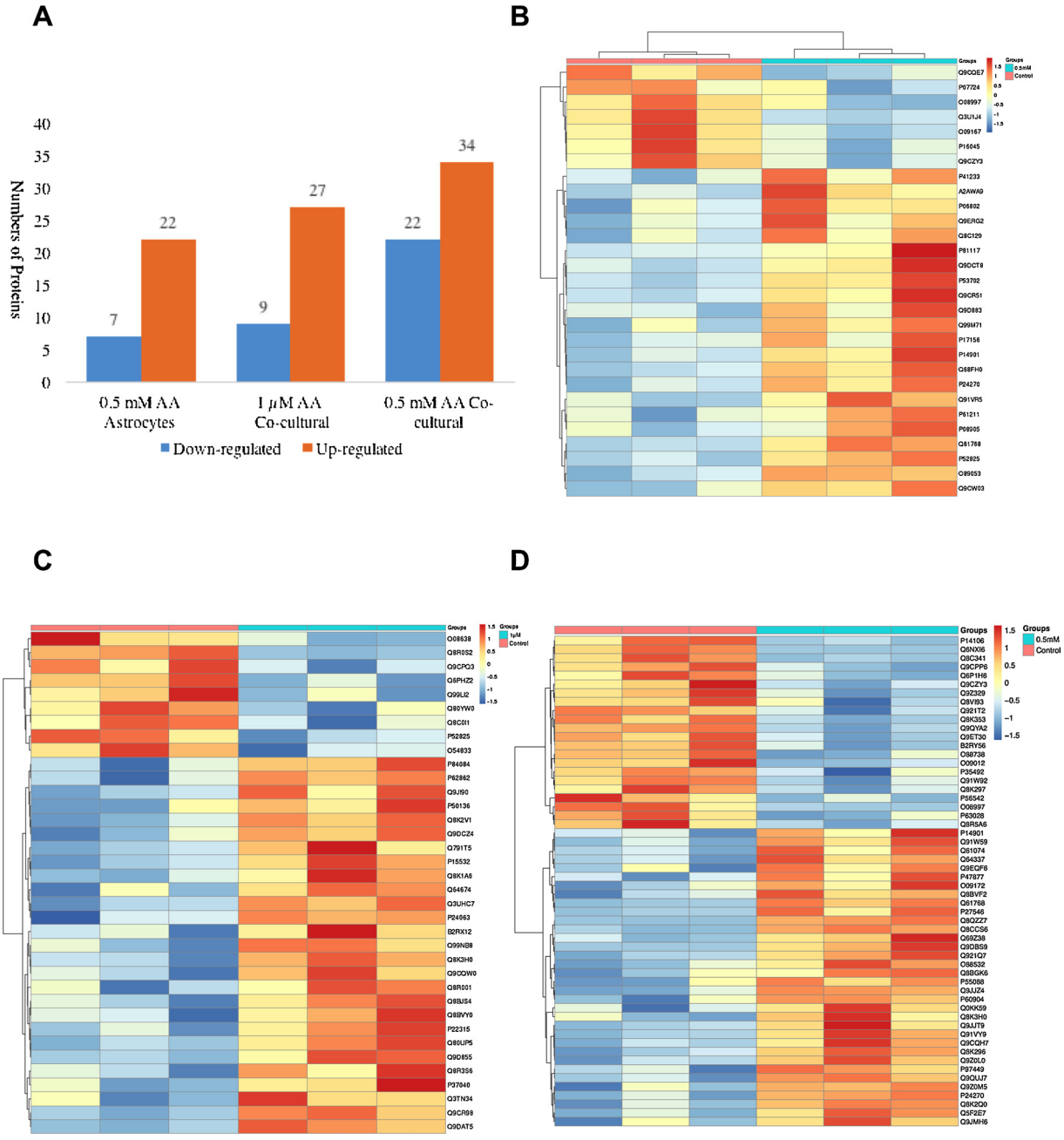

Fig. 2. Differential protein abundance in astrocytes and co-cultured astrocytes/microglia after 24 h of acrylamide (AA) exposure: A. statistical data; heat maps of protein abundance patterns in B. astrocytes exposed to 500 μM AA, C. co-cultured cells exposed to 1 μM AA, and D. co-cultured cells exposed to 500 μM AA.

Table 1
Cellular component distribution of the total identified proteins and differentially expressed proteins in the astrocyte and co-culture acrylamide (AA) treatment groups.

Cell Component (%)	Astrocytes (500 μM AA)	Astrocytes (Total)	Co-culture (1 μM AA)	Co-culture (500 μM AA)	Co-culture (Total)
Membrane	58.6	39.7	47.3	38.9	42.5
Cytoplasm	34.5	29.7	34.6	34.4	32.3
Nucleus	24.1	30.9	25.5	30.0	32.1
Endoplasmic reticulum	6.9	5.4	12.7	12.2	6.8
Mitochondrion	6.9	6.7	23.6	11.1	7.5
Golgi apparatus	3.5	4.7	7.3	6.7	5.4
Microtubule	0	2.1	5.5	4.4	1.9

Cat, Gclm, and Sqstm1, as well as several typical proteins identified in all treatment groups, were further investigated using Western blot analysis to verify the MS results. Among the assessed proteins, Hmox1 was commonly associated with significant elements, especially the terms "response to stimulus" and "cellular and metabolic process." Meanwhile, Atox1 has an important role in cell development, especially in glial and neuronal differentiation (Kelner et al., 2000). Cyto C was selected as a negative control lacking differential expression following AA treatment ($p > 0.05$).

In co-cultured cells, Nrf2, Cat, Gclm, and Sqstm1 showed increased expression ($p < 0.05$) following high dose AA exposure (500 μM), in agreement with the IPA prediction. In line with the MS results, Hmox1 was up-regulated and Atox1 down-regulated in both astrocytes and co-cultured cells exposed to 500 μM AA ($p < 0.05$). No significant changes in Cyto C were evident in any of the treated cultures. All

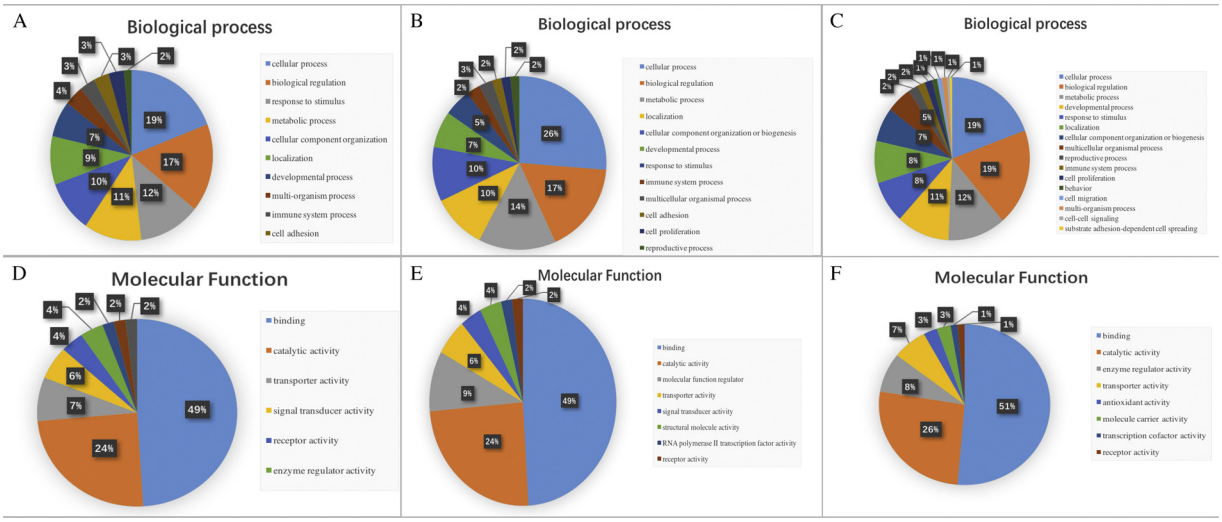

Fig. 3. Enriched GO terms based sets of differentially expressed proteins in acrylamide (AA)-treated astrocytes and co-cultured astrocytes/microglia. Enriched biological processes in A. astrocytes exposed to 500 μM AA, B. co-cultured cells exposed to 1 μM AA, and C. co-cultured cells exposed to 500 μM AA. Enriched molecular functions in D. astrocytes exposed to 500 μM AA, E. co-cultured cells exposed to 1 μM AA, and F. co-cultured cells exposed to 500 μM AA.

Western blot results corresponded with the MS results (Table 2).

4. Discussion

AA is a common food contaminant that develops during the food heating process (Tareke et al., 2002). AA-induced neurotoxicity has been widely investigated in various animal and cell models, including astrocytoma cell lines, primary astrocytes, and BV2 microglial and neuroblastoma cell lines (Lee et al., 2014; Liu et al., 2015; Sumizawa and Igisu, 2007). This is the first study to explore the global proteome changes of AA-induced neurotoxicity using a primary glial cell model and to compare the differences between purified primary astrocytes and primary co-cultures of astrocytes with microglia.

Epidemiological findings suggest that the margin of exposure of AA is approximately 50–200, i.e. average AA consumers had exposure exceeding the tolerable intake of AA by an order of magnitude indicating a potential risk of long term AA exposure (Tardiff et al., 2010). Moreover, the bioaccumulation of AA might affect the human nervous system. Although no cytotoxicity was found in low dose (1 μM) and high dose (500 μM) AA exposure in our study, astrocytes and microglia both displayed cell-specific responses and distinct sensitivity to AA within this exposure range in our previous studies (Zhao et al., 2017a, 2017b). For example, the oxidative stress-related Nrf2 pathway was activated following exposure to 1.0 mM AA for 24 h without significant cell death. In co-cultured astrocytes/microglia, an increase in reactive oxygen species (ROS) formation, decrease in the reduced-to-oxidized glutathione ratio, and activation of Nrf2 and downstream targets (e.g., Hmox1 and glutathione S-transferase) were observed after 24 h of exposure to 0.1–1.0 mM AA, whereas cell viability was not significantly impacted (Zhao et al., 2017a, 2017b). Similarly, Liu et al. (2015) indicated that, although 24 h of exposure to 0.5 mM AA had no effect on viability in BV2 microglial cells, the intrinsic apoptotic pathway was promoted, as was JNK activation (p46). Therefore, despite a lack of significant cytotoxicity, AA exposure can induce related signaling pathways.

In this study, more proteins were differentially expressed after high-dose (500 μM) treatment than low-dose (1 μM) treatment in co-cultured cells, suggesting that toxicity occurred in a dose-dependent manner. Moreover, in the high-dose treatment, more differentially expressed proteins were detected in co-cultured cells than monocultured astrocytes. These results indicated that AA may induce a different biological response in astrocytes in the presence of microglial cells. We cannot ascertain whether this is due to a greater cytotoxicity in astrocytes in the presence of microglial cells, to the contribution of microglial proteins to the total protein set, or to a combination of both. Furthermore, AA treatment might have had specific effects in the endoplasmic reticulum, mitochondrion, golgi apparatus and microtubule in co-cultured cells, suggesting that these organelles are potential targets and might have an essential role in AA neurotoxicity (Table 1). In line with these results, a previous study showed that AA decreased mitochondrial respiration, lowered mitochondrial complex protein expression, and mediated apoptosis in BV2 cells (Liu et al., 2015).

Of the enriched biological regulatory functions, ROS generation was the most significantly affected by AA treatment. Related to ROS generation, the proteins Hmox1, Alb, Cat, and Abca1 were all reportedly influenced by AA toxicity (Fig. 4A). This result corresponded with previous observations in both AA-treated primary cell and animal models (Zhao et al., 2015, 2017a, 2017b). As the other biological regulatory function altered by AA exposure (Pan et al., 2018), the cellular immune response showed significant changes in the interleukin-12 signaling pathway, interleukin-1-mediated signaling pathway, and acute phase response signaling pathway, among others (Fig. 5A). In particular, five differentially expressed proteins were involved in the immune response of cells, among which Hmox1, Cat, Abca1, and Coro1A were up-regulated, whereas Lgals1 was down-regulated (Fig. 4B). These results suggested that AA treatment disrupted the cellular redox balance and elicited an immune response. A previous study reported that AA, much like methylmercury, acted as an electrophile that negatively affected cell morphology and brain structure (Lopachin and Gavin, 2012). Following AA exposure, functional alterations significantly affected ~5% of differentially expressed proteins associated with cell adhesion, cell proliferation, and cellular component organization in all treatment groups. These results were similar to those reported to involve the general effects of AA on glial morphology features and glial differentiation (Shi et al., 2012).

Following a comparison of the two cell cultures, cell-cell signaling alteration and cell migration were only evident in the high-dose AA treatment in the co-cultured model. In particular, the early stages of cellular protrusion formation and microtubule dynamics were activated, and cross-talk was apparent between these two terms, following high-dose AA treatment in co-cultured cells (Fig. 4C). Disruptions in cell-cell communication within glia or among neurons, astrocytes, and microglia have been considered to have a critical role in the development of neurodegenerative diseases. Furthermore, such disruptions

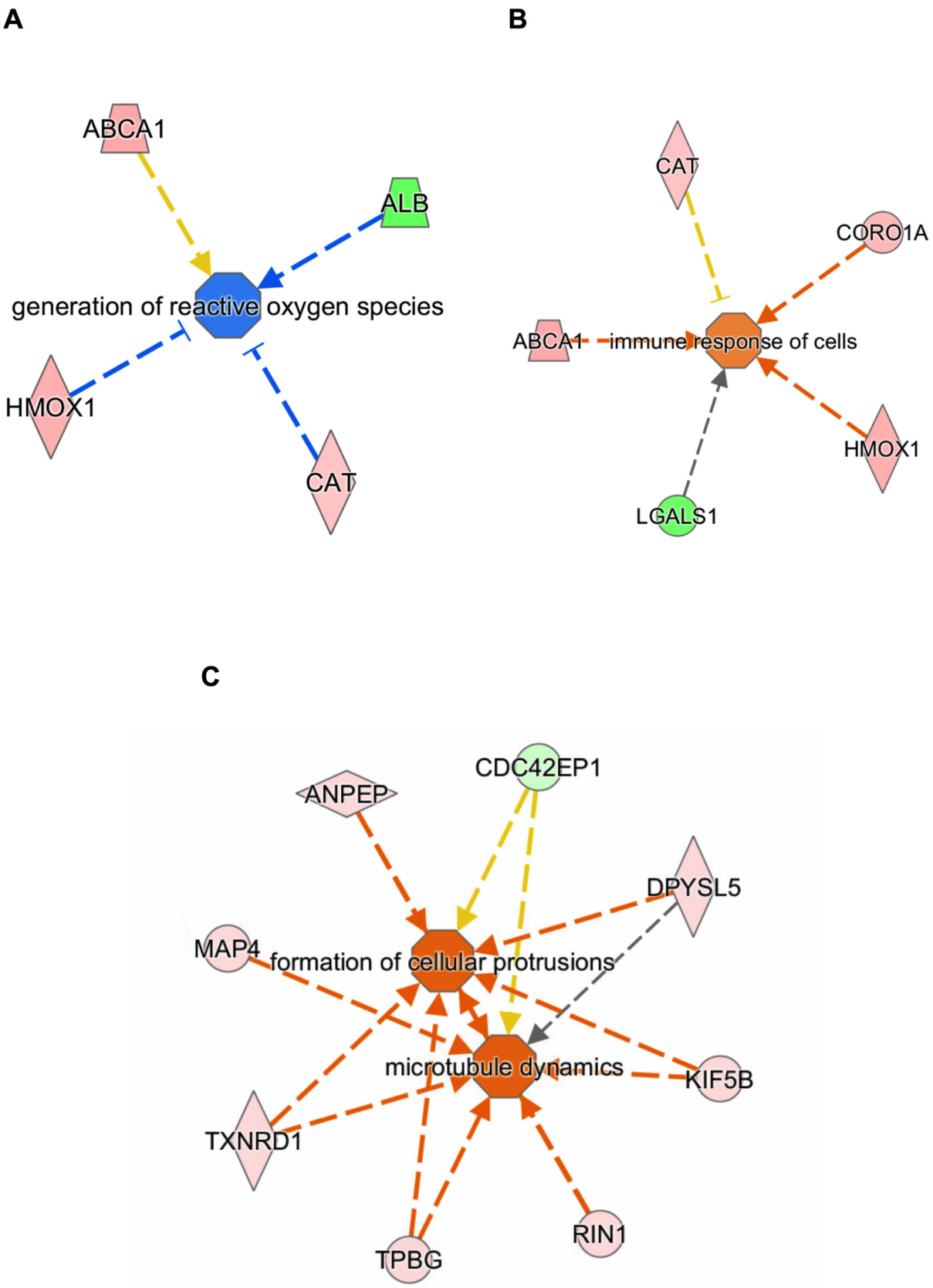

Fig. 4. Functional alterations related to acrylamide (AA) exposure in astrocytes and co-cultured astrocytes/microglia: A. cellular immune response; B. reactive oxygen species generation; and C. cellular protrusion formation and microtubule dynamics.

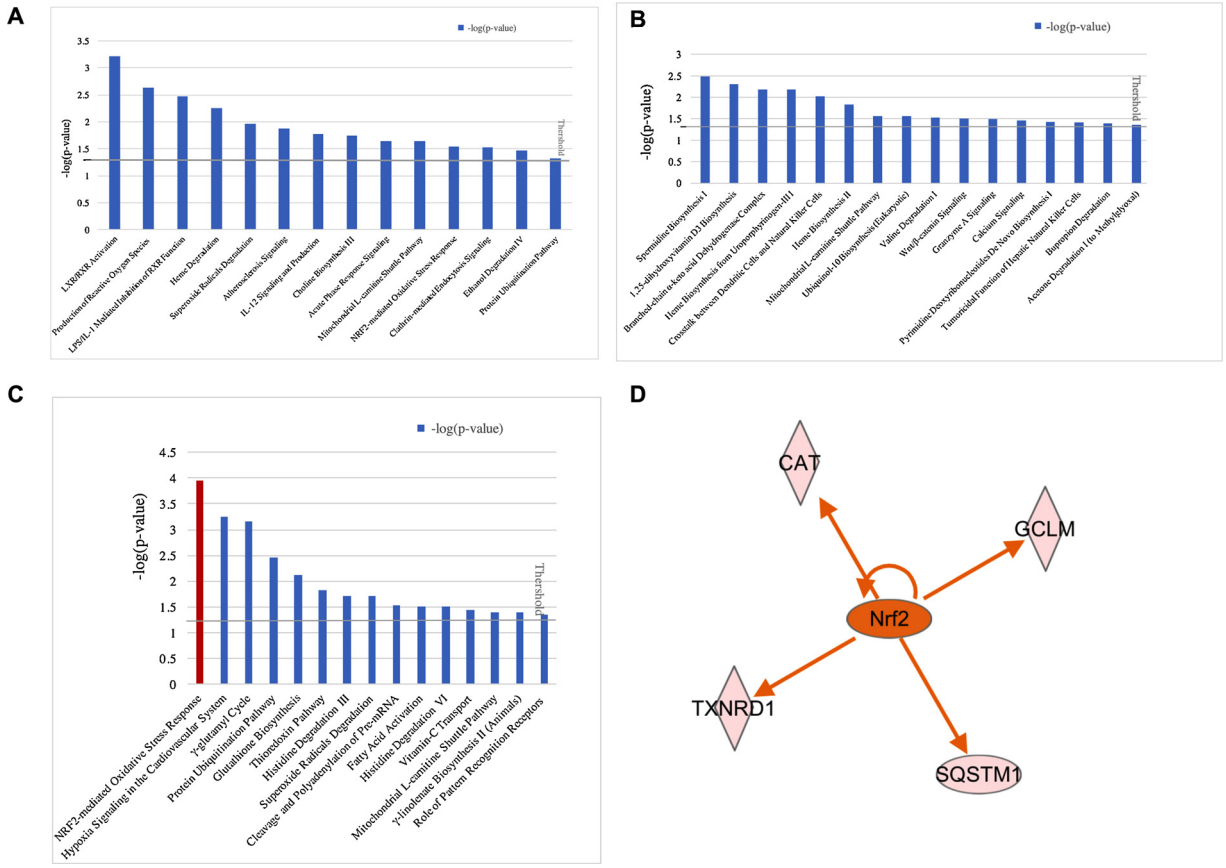

Fig. 5. Canonical pathway alterations related to acrylamide (AA) exposure in astrocytes and co-cultured astrocytes/microglia: A. astrocytes exposed to 500 μM AA, B. co-cultured cells exposed to 1 μM AA, and C. co-cultured cells exposed to 500 μM AA. D. Prediction of the Nrf2 pathway and related downstream proteins. The ratios represent the number of differentially expressed proteins in AA-treated cells to the total number of proteins in each pathway.

affect the initiation and progression of neurotoxicity induced by endo- and xenobiotics, such as CXC chemokine receptor 4, lipopolysaccharides, and *Streptococcus suis* (Bezzi et al., 2001; Gullo et al., 2017; Seele et al., 2016). Astrocytes have a major support function in the central nervous system, as well as a role in inducing microglial activation and differentiation. Meanwhile, microglia defend against oxidative stress and transmit immune signals under inflammation of the central nervous system (Teismann and Schulz, 2004). Rothhammer et al. (2018) reported a detailed mechanism involved in such cellular communication processes. Microglia could control and deactivate astrocytes via TGF-ErbB1 signaling, while reactivating astrocytes via VEGF-B-FLT-1 signaling in an experimental autoimmune encephalomyelitis mouse model. Therefore, in contrast to monocultured astrocytes, these positive and negative microglia regulators induced cell communication, eliciting responses that were more sensitive to specific stimuli. Additionally, the connecting pathways underlying cell-cell signaling were predicted after IPA analysis, involving 11 proteins: Txnrd1, Tpbg, RIN1, Kif5b, Dpysl5, Cdc42ep1, Anpep, Map4, Aqp4, Dnajc5, and Igfbp2. Eight of these proteins shown in Fig. 4C were related to two child terms “cellular protrusion formation” and “microtubule dynamics”. The other three proteins AQP4, DNAJC5, IGFBP2 were related the other child term of “interaction (nervous system development and function)”. Of these proteins, KIF5B assists in intracerebral signaling transmission and acts as the node for cell communication (Ma et al., 2009). Meanwhile, CDC42EP1 controls the formation of membrane protrusions and is critical for efficient migration to the correct location under traction forces (Shlomi et al., 2017). Further research is necessary to confirm these differentially expressed proteins and discuss their connection to the cell communication pathway. Additionally, the differences in the underlying mechanism of toxicity in mono-cultured and co-cultured neural cell models following AA treatment should be explored further.

In this study, IPA predicted the increased expression of Nrf2, which acts as the upstream regulator of Cat, Gclm, and Sqstm1, following AA exposure. Nrf2 is a well-known transcription factor related to oxidative stress, and has shown a feedback relationship with AA-induced neurotoxicity (Zhao et al., 2017a). The MS and IPA results were verified using Western blot analysis, which demonstrated up-regulation of Nrf2, as well as Cat, Gclm, and Sqstm1 (2.9-, 2.2-, and 1.7-fold, respectively) in the high-dose co-culture group. These results suggested that the Nrf2 pathway and related antioxidant genes were involved in AA-induced oxidative stress during the progression of neurotoxicity. Furthermore, Western blot analysis revealed similar variations in Atox1 and Hmox1 in all groups compared with the MS results (Fig. 6B, C and Table 2). Hmox1 had a close relationship with oxidative stress, further highlighting its major role in AA-induced neurotoxicity. These results supported previous findings that Hmox1 significantly increased in both monocultured and co-cultured astrocytes and microglia and following AA treatment (Zhao et al., 2017a, 2017b). Meanwhile, Atox1 is a copper-dependent suppressor of oxidative damage and has been shown to have a crucial role in maintaining brain cell survival and differentiation (Hatori et al., 2016; Kelner et al., 2000). High-dose AA treatment caused down-regulation of Atox1 in both astrocytes and co-cultured cells. This result indicated that AA inhibited the suppression of Atox1 and enhanced oxidative damage in the brain, which could subsequently affect cell differentiation and promote neurotoxicity. These results provide new insights into AA-induced neurotoxicity, helping to clarify the underlying processes and mechanisms. Further investigation of ATOX1 and the related copper homeostasis pathway will be conducted in the future to determine the mechanism of AA-induced neurotoxicity.

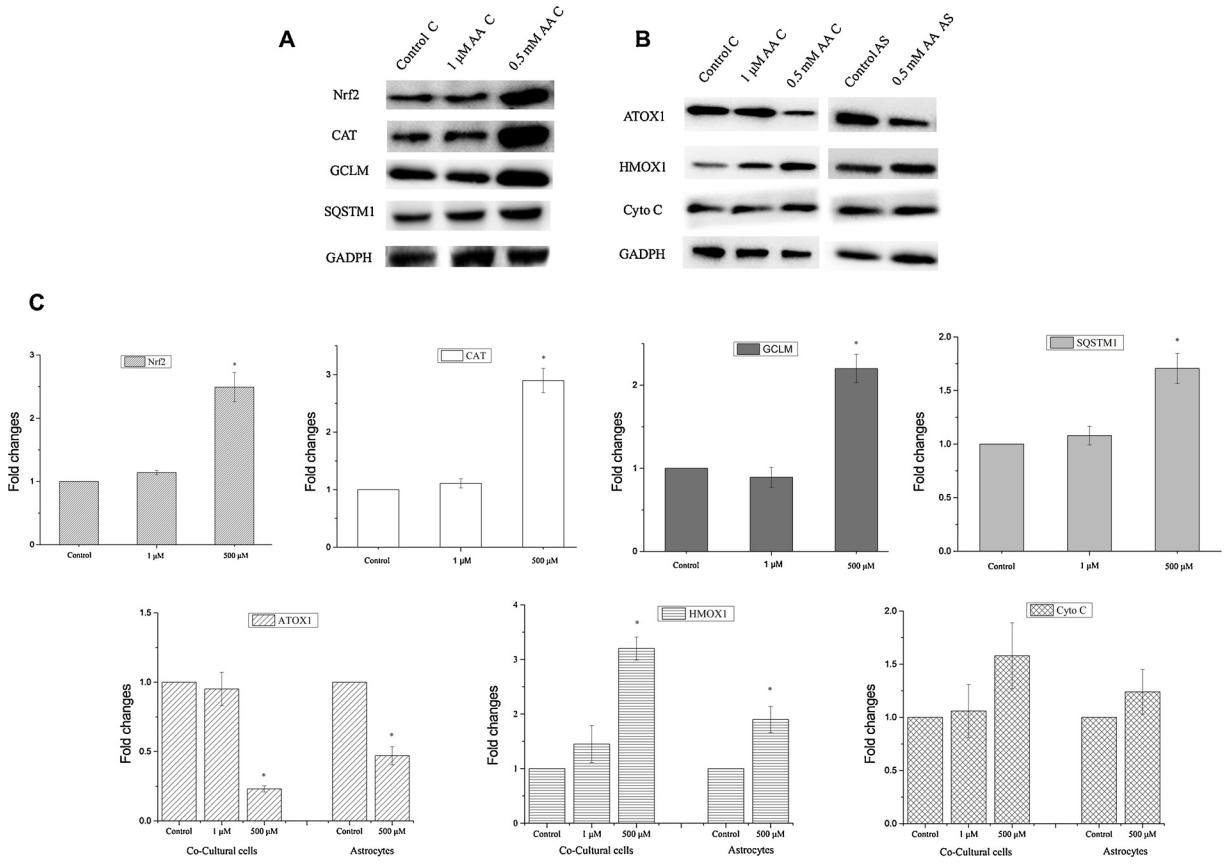

Fig. 6. Western blot analysis for verification of protein expression estimated from the mass spectrometry analysis. A. Representative blots of Nrf2-related proteins in co-cultured cells. B. Representative blots of three selected proteins identified in all treatment groups. C. Expression intensity of the verified proteins. The intensity of each band was quantified by densitometry. AS. Astrocytes; C. Co-cultured astrocytes/microglia. Data are presented as means ± SD of 3 biological-replicates per treatment. * represent a significant difference of $p < 0.05$ between the treatment group with the control group.

Table 2
Comparison of the protein quantification results from the Western blot and proteomics (MS) analyses. AS, astrocyte monoculture; C, astrocyte/microglia co-culture.

Protein ID	Protein Name	Protein Size (kDa)	Fold-change					
			MS			Western Blot		
			500 μM AA, AS	1 μM AA, C	500 μM AA, C	500 μM AA, AS	1 μM AA, C	500 μM AA, C
P14901	HMOX1_MOUSE Heme oxygenase 1	31	2.1	0.97	2.7	1.9	1.45	3.2
O08997	ATOX1_MOUSE Copper transport protein	7	−2.63	−1.1	−4.5	−2.1	−1.05	−4.3
P62897	CYC_MOUSE Cytochrome c_ somatic (negative control)	11	1.43	1.32	2.01	1.24	1.06	1.58

One of the limitations of this study is the lack of information on microglia proteome. This is due to the relatively small amount of microglia cells in the developing brain of the pups; it will require five to ten times the number of mice pups to provide enough microglia cells to complete the experiment. The lack of information on microglia resulted in the ability to distinguish the biological responses between astrocytes and microglia in the co-culture system. Another limitation is the high variability of the biological response and the strict statistical approach used have resulted in a relatively small number of differentially expressed proteins identified, particularly at the low dose treatment group. For example, these have resulted in the detection of 1–2 proteins annotated in each category. Therefore, the results of this study are not conclusive but can serve for hypothesis generation purposes. Further research is necessary to confirm the biological pathways identified.

5. Conclusion

The global effects of AA exposure were examined in mono-cultured astrocyte and co-cultured astrocyte/microglial cell models Using a proteomics approach. The findings revealed that disruption of multicellular metabolic processes, biological regulation, and cell development were the biological functions involved in AA-induced neurotoxicity. In particular, oxidative stress-related pathways and immune response signaling were primarily affected in both high-dose groups. The Nrf2 pathway and downstream proteins Hmox1, Cat, Gclm, and Sqstm1 were crucial targets associated with oxidative stress related to AA neurotoxicity. Atox1, involved in copper homeostasis, was another potential target. In the co-cultured cell model, cell communication and morphogenesis, especially the early stages of cellular protrusion formation and microtubule dynamics, were significantly altered by AA exposure. These functional and pathway modifications provide new

insights for the development of an alternative pathway approach for the risk assessment of AA. Further study of these targets will improve the understanding of the pathogenesis of AA neurotoxicity.

Conflict of interest

The authors declare that there are no conflicts of interest.

Declaration of Competing Interest

The authors declare that they have no conflict of interest.

Acknowledgments

Mengyao Zhao was the recipient of a China Government Scholarship from the China Scholarship Council. This work was supported by the National Natural Science Foundation of China [31801668]; the Canada Research Chair Program to HMC; and the Shanghai Pujiang Program [18J1401900]. We thank Dr. Gleb Mironov and Dr. Maxim Berezovski of the John L. Holmes Mass Spectrometry Facility at the University of Ottawa for their technical support with the liquid chromatography-mass spectrometry analysis.

Appendix A. Supplementary data

Supplementary material related to this article can be found, in the online version, at doi:https://doi.org/10.1016/j.neuro.2019.09.005.

References

Abelli, L., Ferri, G.L., Astolfi, M., Conte, B., Geppetti, P., Parlani, M., Dahl, D., Polak, J.M., Maggi, C.A., 1991. Acrylamide-induced visceral neuropathy: evidence for the involvement of capsaicin-sensitive nerves of the rat urinary bladder. Neuroscience 41, 311–321.

Anderson, C.M., Swanson, R.A., 2000. Astrocyte glutamate transport: review of properties, regulation, and physiological functions. Glia 32, 1–14.

Barber, D.S., LoPachin, R.M., 2004. Proteomic analysis of acrylamide-protein adduct formation in rat brain synaptosomes. Toxicol. Appl. Pharmacol. 201, 120–136. https://doi.org/10.1016/j.taap.2004.05.008.

Barber, D.S., Stevens, S., LoPachin, R.M., 2007. Proteomic analysis of rat striatal synaptosomes during acrylamide intoxication at a low dose rate. Toxicol. Sci. 100, 156–167. https://doi.org/10.1093/toxsci/kfm210.

Basile, A., Ferranti, P., Moccaldi, R., Spagnoli, G., Sannolo, N., 2008. Proteomic approach for the analysis of acrylamide-hemoglobin adducts. Perspectives for biological monitoring. J. Chromatogr. A 1215, 74–81. https://doi.org/10.1016/j.chroma.2008.10.093.

Bezzi, P., Domercq, M., Brambilla, L., Galli, R., Schols, D., De Clercq, E., Vescovi, A., Bagetta, G., Kollias, G., Meldolesi, J., Volterra, A., 2001. CXCR4-activated astrocyte glutamate release via TNFα: amplification by microglia triggers neurotoxicity. Nat. Neurosci. 4, 702.

Caito, S.W., Yu, Y., Aschner, M., 2014. Differential inflammatory response to acrylonitrile in rat primary astrocytes and microglia. NeuroToxicology 42, 1–7.

Calleman, C.J., Wu, Y., He, F., Tian, G., Bergmark, E., Zhang, S., Deng, H., Wang, Y., Crofton, K.M., Fennell, T., Costa, L.G., 1994. Relationships between biomarkers of exposure and neurological effects in a group of workers exposed to acrylamide. Toxicol. Appl. Pharm. 126, 361–371.

Doerge, D.R., Gamboa da Costa, G., McDaniel, L.P., Churchwell, M.I., Twaddle, N.C., Beland, F.A., 2005. DNA adducts derived from administration of acrylamide and glycidamide to mice and rats. Mutat. Res. 580, 131–142.

Edwards, P., Sporel-Ozakat, R., Gispen, W., 1991. Peripheral pain fiber function is relatively insensitive to the neurotoxic actions of acrylamide in the rat. Toxicol. Appl. Pharmacol. 111, 43–48.

Fullerton, P.M., 1969. Electrophysiological and histological observations on peripheral nerves in acrylamide poisoning in man. J. Neurol. Neurosurg. Psychiatry 32, 186–192. https://doi.org/10.1136/jnnp.32.3.186.

Ghanayem, B.I., McDaniel, L.P., Churchwell, M.I., Twaddle, N.C., Snyder, R., Fennell, T.R., Doerge, D.R., 2005. Role of CYP2E1 in the epoxidation of acrylamide to glycidamide and formation of DNA and hemoglobin adducts. Toxicol. Sci. 88, 311–318. https://doi.org/10.1093/toxsci/kfi307.

Gullo, F., Ceriani, M., D'Aloia, A., Wanke, E., Constanti, A., Costa, B., Lecchi, M., 2017. Plant polyphenols and exendin-4 prevent hyperactivity and TNF-α release in LPS-treated in vitro neuron/astrocyte/microglial networks. Front. Neurosci. 11, 1–13. https://doi.org/10.3389/fnins.2017.00500.

Hatori, Y., Yan, Y., Schmidt, K., Furukawa, E., Hasan, N.M., Yang, N., Liu, C.N., Sockanathan, S., Lutsenko, S., 2016. Neuronal differentiation is associated with a redox-regulated increase of copper flow to the secretory pathway. Nat. Commun. 7, 1–12. https://doi.org/10.1038/ncomms10640.

Huang, Y.F., Chiang, S.Y., Liou, S.H., Chen, M.L., Chen, M.F., Uang, S.N., Wu, K.Y., 2012. The modifying effect of CYP2E1, GST, and mEH genotypes on the formation of hemoglobin adducts of acrylamide and glycidamide in workers exposed to acrylamide. Toxicol. Lett. 215, 92–99. https://doi.org/10.1016/j.toxlet.2012.10.003.

International Agency for Research on Cancer (IARC), 1994. IARC Monographs on the Evaluation of Carcinogen Risk to Human: Some Industrial Chemicals. Lyon.

Kelner, G.S., Lee, M., Clark, M.E., Maciejewski, D., McGrath, D., Rabizadeh, S., Lyons, T., Bredesen, D., Jenner, P., Maki, R.A., 2000. The copper transport protein Atox1 promotes neuronal survival. J. Biol. Chem. 275, 580–584. https://doi.org/10.1074/jbc.275.1.580.

Kuhlmann, A.C., Guilarte, T.R., 2000. Cellular and subcellular localization of peripheral benzodiazepine receptors after trimethyltin neurotoxicity. J. Neurochem. 74, 1694–1704.

Kütting, B., Schettgen, T., Schwegler, U., Fromme, H., Uter, W., Angerer, H., Drexler, H., 2009. Acrylamide as environmental noxious agent: a health risk assessment for the general population based on the internal acrylamide burden. Int. J. Hyg. Environ. Health 213, 470–480.

Lakshmi, D., Gopinath, K., Jayanthy, G., Anjum, S., Prakash, D., Sudhandiran, G., 2012. Ameliorating effect of fish oil on acrylamide induced oxidative stress and neuronal apoptosis in cerebral cortex. Neurochem. Res. 37, 1859–1867. https://doi.org/10.1007/s11064-012-0794-1.

Lee, J.G., Wang, Y.S., Chou, C.C., 2014. Acrylamide-induced apoptosis in rat primary astrocytes and human astrocytoma cell lines. Toxicol. In Vitro 28, 562–570.

Liu, Z., Song, G., Zou, C., Liu, G., Wu, W., Yuan, T., Liu, X., 2015. Acrylamide induces mitochondrial dysfunction and apoptosis in BV-2 microglial cells. Free Radic. Biol. Med. 84, 42–53. https://doi.org/10.1016/j.freeradbiomed.2015.03.013.

Long, T.C., Tajuba, J., Sama, P., Saleh, N., Swartz, C., Parker, J., Hester, S., Lowry, G.V., Veronesi, B., 2007. Nanosize titanium dioxide stimulates reactive oxygen species in brain microglia and damages neurons in vitro. Env. Heal. Persp. 115, 1631–1637.

LoPachin, R.M., Barber, D.S., 2006. Synaptic cysteine sulfhydryl groups as targets of electrophilic neurotoxicants. Toxicol. Sci. 94, 240–255. https://doi.org/10.1093/toxsci/kfl066.

Lopachin, R.M., Gavin, T., 2012. Molecular mechanism of acrylamide neurotoxicity: lessons learned from organic chemistry. Env. Heal. Persp. 120, 1650–1657.

Ma, H., Cai, Q., Lu, W., Sheng, Z.-H., Mochida, S., 2009. KIF5B motor adaptor syntabulin maintains synaptic transmission in sympathetic neurons. J. Neurosci. 29, 13019–13029. https://doi.org/10.1523/JNEUROSCI.2517-09.2009.

Marek, R., Caruso, M., Rostami, A., Grinspan, J.B., Sarma, J.D., 2008. Magnetic cell sorting: a fast and effective method of concurrent isolation of high purity viable astrocytes and microglia from neonatal mouse brain tissue. J. Neurosci. Meth. 175, 108–118.

Martyniuk, C.J., Feswick, A., Fang, B., Koomen, J.M., Barber, D.S., Gavin, T., LoPachin, R.M., 2013. Protein targets of acrylamide adduct formation in cultured rat dopaminergic cells. Toxicol. Lett. 219, 279–287. https://doi.org/10.1016/j.toxlet.2013.03.031.

Mottram, D.S., Wedzicha, B.L., Dodson, A.T., 2002. Acrylamide is formed in the Maillard reaction. Nature 419, 448–449.

Ni, M., Li, X., Yin, Z., Sidoryk-Węgrzynowicz, M., Jiang, H., Farina, M., Rocha, J.B.T., Syversen, T., Aschner, M., 2011. Comparative study on the response of rat primary astrocytes and microglia to methylmercury toxicity. Glia 59, 810–820.

Pan, X., Wu, X., Yan, D., Peng, C., Rao, C., Yan, H., 2018. Acrylamide-induced oxidative stress and inflammatory response are alleviated by N-acetylcysteine in PC12 cells: involvement of the crosstalk between Nrf2 and NF-κB pathways regulated by MAPKs. Toxicol. Lett. 288, 55–64. https://doi.org/10.1016/j.toxlet.2018.02.002.

Pan, X., Yan, D., Wang, D., Wu, X., Zhao, W., Lu, Q., Yan, H., 2017. Mitochondrion-mediated apoptosis induced by acrylamide is regulated by a balance between Nrf2 antioxidant and MAPK signaling pathways in PC12 Cells. Mol. Neurobiol. 54, 4781–4794. https://doi.org/10.1007/s12035-016-0021-1.

Prasad, S.N., Muralidhara, M., 2013. Neuroprotective efficacy of eugenol and isoeugenol in acrylamide-induced neuropathy in rats: behavioral and biochemical evidence. Neurochem. Res. 38, 330–345. https://doi.org/10.1007/s11064-012-0924-9.

Prasad, S.N., Muralidhara, M., 2014. Mitigation of acrylamide-induced behavioral deficits, oxidative impairments and neurotoxicity by oral supplements of geraniol (a monoterpene) in a rat model. Chem. Biol. Interact. 223, 27–37. https://doi.org/10.1016/j.cbi.2014.08.016.

Rabilloud, T., Lescuyer, P., 2015. Proteomics in mechanistic toxicology: history, concepts, achievements, caveats, and potential. Proteomics 15, 1051–1074. https://doi.org/10.1002/pmic.201400288.

Ralevic, V., Aberdeen, J.A., Burnstock, G., 1991. Acrylamide-induced autonomic neuropathy of rat mesenteric vessels: histological and pharmacological studies. J. Auton. Nerv. Syst. 34, 77–87.

Rothhammer, V., Borucki, D.M., Tjon, E.C., Takenaka, M.C., Chao, C., Ardura-fabregat, A., Lima, K.A., De Gutiérrez-vázquez, C., Hewson, P., Staszewski, O., Blain, M., Healy, L., Neziraj, T., Borio, M., Wheeler, M., Dragin, L.L., Laplaud, D.A., Antel, J., Alvarez, J.I., Prinz, M., Quintana, F.J., 2018. Microbial control of astrocytes in response to microbial metabolites. Nature 557, 724–728. https://doi.org/10.1038/s41586-018-0119-x.

Seele, J., Nau, R., Prajeeth, C.K., Stangel, M., Valentin-Weigand, P., Seitz, M., 2016. Astrocytes enhance streptococcussuis-glial cell interaction in primary astrocyte-microglial cell co-cultures. Pathogens 5, 1–13. https://doi.org/10.3390/pathogens5020043.

Shi, J., Ma, Y., Zheng, M., Ruan, Z., Liu, J., Tian, S., Zhang, D., He, X., Li, G., 2012. Effect of sub-acute exposure to acrylamide on GABAergic neurons and astrocytes in weaning rat cerebellum. Toxicol. Ind. Health 28, 10–20. https://doi.org/10.1177/0748233711401264.

Shlomi, C., Kovari, D.T., Wei, W., Keate, R., Curtis, J.E., Nie, S., 2017. Cdc42 regulates the cellular localization of Cdc42ep1 in controlling neural crest cell migration. J. Mol. Cell Biol. 1–12. https://doi.org/10.1093/jmcb/mjx044.

Stadler, R.H., Blank, I., Varga, N., 2002. Acrylamide from Maillard reaction products. Nature 419, 449–450.

Streit, W.J., Graeber, M.B., Kreutzberg, G.W., 1998. Functional plasticity of microglia: a review. Glia 1, 301–307.

Sumizawa, T., Igisu, H., 2007. Apoptosis induced by acrylamide in SH-SY5Y cells. Arch. Toxicol. 81, 279–282. https://doi.org/10.1007/s00204-006-0145-6.

Tardiff, R., Gargas, M., Kirman, C., Carson, M., Sweeney, L., 2010. Estimation of safe dietary intake levels of acrylamide for humans. Food Chem. Toxicol. 48, 658–667.

Tareke, E., Rydberg, P., Karlsson, P., Eriksson, S., Tornqvist, M., 2002. Analysis of acrylamide, a carcinogen formed in heated foodstuffs. J. Agric. Food Chem. 50, 4998–5006.

Tareke, E., Twaddle, N.C., McDaniel, P., Churchwell, M.I., Young, J.F., Doerge, D.R., 2006. Relationships between biomarkers of exposure and toxicokinetics in Fischer 344 rats and B6C3F1 mice administered single doses of acrylamide and glycidamide and multiple doses of acrylamide. Toxicol. Appl. Pharmacol. 217, 63–75.

Teismann, P., Schulz, J.R.B., 2004. Cellular pathology of Parkinson's disease: astrocytes, microglia and inflammation. Cell Tissue Res. 318, 149–161.

Zhang, Y., Ren, Y., Zhang, Y., 2009. New research developments on acrylamide analytical chemistry, formation mechanism, and mitigation recipes. Chem. Rev. 109, 4375–4397.

Zhao, M., Lewis Wang, F.S., Hu, X., Chen, F., Chan, H.M., 2017a. Acrylamide-induced neurotoxicity in primary astrocytes and microglia: roles of the Nrf2-ARE and NF-κB pathways. Food Chem. Toxicol. 106, 25–35. https://doi.org/10.1016/j.fct.2017.05.007.

Zhao, M., Wang, F.S.L., Hu, X.S., Chen, F., Chan, H.M., 2017b. Effect of acrylamide-induced neurotoxicity in a primary astrocytes/microglial co-culture model. Toxicol. In Vitro 39, 119–125. https://doi.org/10.1016/j.tiv.2016.11.007.

Zhao, M., Wang, P., Zhu, Y., Liu, X., Hu, X., Chen, F., 2015. The chemoprotection of a blueberry anthocyanin extract against the acrylamide-induced oxidative stress in mitochondria: unequivocal evidence in mice liver. Food Funct. 6, 3006–3012. https://doi.org/10.1039/C5FO00408J.